

Quantum Kinetic Anatomy of Electron Angular Momenta Edge Accumulation

Thierry Valet,^{1,*} Henri Jaffrès,² Vincent Cros,² and Roberto Raimondi³

¹*MPhysX OÜ, Harju maakond, Tallinn, Lasnamäe linnaosa, Sepapaja tn 6, 15551, Estonia*

²*Laboratoire Albert Fert, CNRS, Thales, Université Paris-Saclay, 91767 Palaiseau, France*

³*Dipartimento di Matematica e Fisica, Università Roma Tre, Via della Vasca Navale 84, 00146 Roma, Italy*

(Dated: July 10, 2025)

Controlling electron’s spin and orbital degrees of freedom has been a major research focus over the past two decades, as it underpins the electrical manipulation of magnetization. Leveraging a recently introduced quantum kinetic theory of multiband systems [T. Valet and R. Raimondi, *Phys. Rev. B* 111, L041118 (2025)], we outline how the intrinsic angular momenta linear response is partitioned into intraband and interband contributions. Focusing on time reversal and inversion symmetric metals, we show that the spin and orbital Hall currents are purely intraband. We also reveal that the edge densities originate partially, and in the orbital case mostly, from a new interband mechanism. We discuss how this profoundly impacts the interpretation of orbital edge accumulation observations, and has broader implications for our understanding of current induced torques.

Electrical generation of out-of-equilibrium spin angular momentum (SAM) and orbital angular momentum (OAM) in nonmagnetic materials are central phenomena in the fields of spin-orbitronics [1, 2] and orbitronics [3, 4], respectively. The growing interest and rapid progress in these areas are largely driven by their potential to manipulate magnetization [5–9, & references therein]. Intrinsic angular momentum (AM) transverse current response in time reversal (TR) and inversion (I) symmetric metals continue to be a central focus. Early work concentrated on heavy *5d* metals (*e.g.*, Pt, Ta or W), where strong spin-orbit interaction (SOI) gives rise to a large, theoretically predicted, intrinsic spin Hall effect (SHE) [10, 11]. More recently, interest has shifted to light elements with weak SOI (*e.g.*, Ti, Cr, V or Mn), spurred by predictions of a “giant” intrinsic orbital Hall effect (OHE), remarkably found independent of the SOI [12–17]. Observations of spin edge accumulation (SEA) [18, 19] and orbital edge accumulation (OEA) [20–22], at the boundaries of thin-film elemental-metal conductors are widely regarded as the most direct experimental confirmations of the predicted intrinsic SHE and OHE, respectively. This interpretation relies on analysis assuming diffusive transport of X angular momentum (XAM) – with X denoting either spin (S) or orbital (O) – in which the intrinsic X Hall effect (XHE) is treated as a source term [18, 21].

In this Letter, we present a unified quantum kinetic theory of the intrinsic XHE and X edge accumulation (XEA) in metals with (TR+I) symmetry. Departing from previous theoretical approaches, we demonstrate that the physically relevant XHE corresponds to the transverse current of the *band projected* XAM. Except in (rare) cases of orbital degeneracy [3], this leads to the conclusion that the intrinsic OHE is second order in the SOI. As another key result, we uncover a novel contribution to the XEA stemming from gradients in the intraband longitudinal response. These gradients *locally*

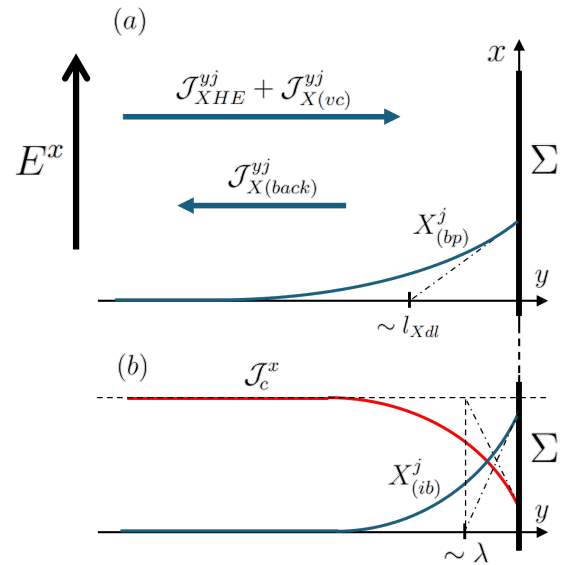


FIG. 1. Near a boundary Σ of a (TR+I) symmetric metal conductor, a tangential electric field E^x is inducing XEA. (a) The band projected part $X_{(bp)}^j$, is confined within a few XAM diffusion lengths l_{Xdl} , resulting from the detailed balance between the intrinsic XHE current with vertex correction $J_{XHE}^{yj} + J_{X(vc)}^{yj}$, the backflow current $J_{X(back)}^{yj}$ and the XAM relaxation. (b) The interband part $X_{(ib)}^j$, is confined within a few electron mean free paths λ . It results from quantum coherences induced by the transverse gradient in the longitudinal response, which also manifests itself by a decreased charge current density J_c^x near the edge.

generate interband coherences – a general effect recently predicted by Valet and Raimondi [23]– and naturally arise near conductor boundaries [24–26]. A concrete calculation for an often considered prototypical model of (TR+I) symmetric metals [27–29] reveals that this can be seen as *XAM-vorticity coupling* locally induced by virtual interband transitions. While this new effect likely dominates the OEA in metals with weak SOI, it has broader implications for our understanding of current induced torques, opening new perspectives for the fields of spin-orbitronics and orbitronics.

* Corresponding author : tvalet@mphysx.com

We consider a generic crystal exhibiting (TR+I) symmetry, whose electronic structure in the vicinity of the Fermi level is assumed to be well approximated by a low energy Hamiltonian $\hat{h}(\mathbf{p}) = \sum_n \varepsilon_n \hat{P}_n$, with \mathbf{p} the kinetic pseudo-momentum, n the band index, ε_n the band energies and \hat{P}_n the associated eigenprojectors [30, 31]. Excluding any rare orbital degeneracies beyond Kramers' theorem, we focus on the generic case in which each band is twofold degenerate under the assumed symmetry. We introduce the single-particle observable $\hat{\mathbf{X}} \equiv \hat{X}^j$, with the index j labeling its different spatial components. This observable stands for either the spin $\hat{\mathbf{S}}$ or the OAM $\hat{\mathbf{L}}$, as appropriate. As for any other operator in the considered Hilbert space, the XAM operator can be *uniquely* decomposed as $\hat{\mathbf{X}} = \hat{\mathbf{X}}_{(bp)} + \hat{\mathbf{X}}_{(ib)}$, where $\hat{\mathbf{X}}_{(bp)} = \sum_n \hat{P}_n \hat{\mathbf{X}} \hat{P}_n = \sum_n \hat{\mathbf{X}}_n$ is the band-projected part, and $\hat{\mathbf{X}}_{(ib)} = \sum_{n \neq m} \hat{P}_n \hat{\mathbf{X}} \hat{P}_m = \sum_{n \neq m} \hat{\mathbf{X}}_{nm}$ carries the interband contributions. This decomposition follows directly from the completeness relation of the projectors. We are interested in the expectation value $\mathbf{X} \equiv \langle \hat{\mathbf{X}} \rangle$, evaluated in linear response to an electric field \mathbf{E} which we assume to be quasi-uniform and slowly varying in time. Building on our recent quantum kinetic theory of multiband systems [23, 32], and as detailed in the Supplemental Material [33], we obtain a continuity equation for the band-projected part

$$\partial_t X_{(bp)}^j + \partial_i \mathcal{J}_X^{ij} = \partial_t X_{(bp)}^j |_{(relax)}, \quad (1)$$

which *defines* the XAM current \mathcal{J}_X^{ij} . The right-hand-side (RHS) captures the disorder induced XAM relaxation processes. As for the interband part, it is determined by the field induced quantum coherences. It reads

$$\mathbf{X}_{(ib)} = \sum_{n \neq m} \int_{BZ} \frac{d^d p}{(2\pi\hbar)^d} \text{Tr} \left[\hat{\rho}_{nm} \hat{\mathbf{X}}_{mn} \right], \quad (2)$$

where the integration in the momentum space of dimension d extends over the Brillouin zone (BZ). A general expression of the band off-diagonal elements of the density matrix, *i.e.*, $\hat{\rho}_{nm}$, has been derived in [23], where it is thoroughly established that these interband coherences are *locally* induced quantities – and consequently, so is $\mathbf{X}_{(ib)}$. This local character implies that *no long range XAM current* is associated with the interband contribution. Therefore, the physical XAM current can be identified with \mathcal{J}_X^{ij} as defined by Eq.(1). It comprises three distinct contributions

$$\mathcal{J}_X^{ij} = \mathcal{J}_{XHE}^{ij} + \mathcal{J}_{X(vc)}^{ij} + \mathcal{J}_{X(back)}^{ij}. \quad (3)$$

The first term is the *intrinsic* XHE current which reads

$$\mathcal{J}_{XHE}^{ij} = -e\hbar \epsilon_{ikl} E^k \sum_n \int_{BZ} \frac{d^d p}{(2\pi\hbar)^d} n_{FD}(\varepsilon_n) \text{Tr} \left[\hat{X}_n^j \hat{\mathcal{F}}_n^l \right], \quad (4)$$

with ϵ_{ikl} the Levi-Civita symbol, and with the integration being carried over the occupied states in equilibrium,

as determined by the Fermi-Dirac distribution n_{FD} . We find the intrinsic XHE current to be governed by the vector Berry curvature $\hat{\mathcal{F}}_n^l = (\hat{\mathcal{F}}_n)^l = (1/2)\epsilon_{lab}\hat{\mathcal{F}}_n^{ab}$, with $\hat{\mathcal{F}}_n^{ab} = i\hat{P}_n[\partial_p^a \hat{P}_n, \partial_p^b \hat{P}_n]_{(-)}\hat{P}_n$, the non-Abelian Berry curvature tensor and $[\cdot, \cdot]_{(-)}$ denoting a commutator. While an equivalent expression has been previously obtained in the SHE case using the wave-packet formalism [34, 35], our derivation provides for the first time a rigorous first principle formulation of the more general intrinsic XHE, from a controlled semiclassical expansion of the Keldysh theory. Furthermore, it is to be emphasized that most recent theoretical studies incorrectly evaluate the intrinsic XHE current as the expectation value, taken from the Fermi sea term of the Kubo formula, of the conventional XAM current operator, *i.e.*, $\hat{\mathcal{J}}_{X(conv)}^{ij} = \frac{1}{2}[\partial_{p^i} \hat{h}, \hat{X}^j]_{(+)}$, in which $[\cdot, \cdot]_{(+)}$ denotes an anti-commutator. This seems to be solely based on an unfounded analogy with the Kubo formula for the intrinsic anomalous Hall effect (AHE), and lacks rigorous justification. It leads to the introduction of the so-called spin and orbital Berry curvatures, which are nonphysical and shall not be mistaken for the non-Abelian Berry curvature $\hat{\mathcal{F}}_n$ truly controlling the XHE. Interestingly, the continued use of this method persists despite the fact that the seminal works of Murakami *et al* [36] on SHE theory, and of Bernevig *et al* [3] on OHE theory, had already outlined two decades ago that the conventional XAM current operators are not physical. The alternative definition of conserved currents proposed in [3, 36], given by the expectation value of $\hat{\mathcal{J}}_{X(cons)}^{ij} = \frac{1}{2}[\partial_{p^i} \hat{h}, \hat{X}_{(bp)}^j]_{(+)}$, while an appealing concept, still lacks a rigorous justification and does not generally lead to a correct evaluation of the intrinsic XHE current as given by our Eq.(4). In the spin case, and although different definitions of the current can lead to quantitative differences in predicted values of the intrinsic SHE conductivity [37], the qualitative conclusion that the intrinsic SHE is first order in the SOI strength is unaffected. In contrast, for the orbital case, an appropriate definition of the current is crucial. The conventional current choice leads to the erroneous conclusion that the intrinsic OHE in light transition metals is independent of the SOI. Our Eq.(4) establishes that in (TR+I) symmetric metals, and in the absence of exceptional orbital degeneracy, the intrinsic OHE is at least second order in the SOI. This is because both the intraband part of the OAM operator and the non-Abelian Berry curvature vanish in the zero SOI limit under the stated hypothesis [33]. Finally, even when focusing on the intrinsic XHE, one must account for the potential contribution of disorder induced vertex corrections, which corresponds to the second term in Eq.(3). While such corrections have been considered before in the contexts of the intrinsic SHE and OHE, these analyses were based on the conventional or conserved current operator definitions [29, 36]. Consequently, this has to be re-evaluated within the present framework. We outline in the Supplemental Material [33] the procedure to derive an explicit expression for the vertex correction to the physical intrinsic XHE current.

Switching our attention to the XEA, we consider now a finite system, with an electric field applied parallel to one of its boundaries Σ , as illustrated in Fig.(1). This configuration generally gives rise to a non-zero XEA, *i.e.*, a steady state XAM density X^j in the vicinity of Σ . We first focus on its band projected part, whose spatial gradient is linked to the backflow current $\mathcal{J}_{X^{(back)}}^{ij}$, *i.e.*, the third term on the RHS of Eq.(3). To obtain a closed formulation for $X_{(bp)}^j$, the following elements are needed : (i) an explicit form for the relaxation term on the RHS of Eq.(1), for instance $\partial_t X_{(bp)}^j|_{(relax)} = -(\bar{\tau}_X^{-1})^j{}_i X_{(bp)}^i$, with $\bar{\tau}_X$ the XAM relaxation time tensor, (ii) the determination of the XAM diffusion tensor \bar{D}_X so that $\mathcal{J}_{X^{(back)}}^{ij} = -\bar{D}_X^{ijk} \partial_k X_{(bp)}^l$, and (iii) the specification of the boundary conditions on Σ , for instance with the introduction of an XAM relaxation velocity tensor \bar{V} , leading to $n_i \mathcal{J}_X^{ij}|_{\Sigma} = \bar{V}^{ij}{}_k X_{(bp)}^k|_{\Sigma}$, with $\mathbf{n} \equiv n^i$ the local outgoing normal vector at the boundary. Such parameterization allows for a varying degree of conservation of the XAM at the boundary. A vanishing \bar{V} corresponds to perfect XAM conservation and maximum XEA, while an infinite relaxation velocity corresponds to perfect absorption of the incoming XAM current and vanishing XEA. Assuming isotropic relaxation and diffusion for simplicity, one can derive (iv) the diffusion equation $\Delta X_{(bp)}^i = X_{(bp)}^i / l_{Xdl}^2$, with Δ the Laplacian and $l_{Xdl} = \sqrt{D_X \tau_X}$ the XAM diffusion length that sets the spatial extent of the band-projected part of the XEA. This diffusive transport framework aligns with the common models used to analyze XEA experiments, and is illustrated in Fig.1(a). While our quantum kinetic framework is ideally suited for deriving microscopic expressions for the transport parameters introduced in (i-iv), we choose not doing it here, as this lies within the scope of established phenomenology. Importantly, as we have shown, the XHE-related XEA only capture the band projected contribution to the total XEA and thus does not provide a complete description.

We identify a novel contribution to the XEA that is confined within a few electron mean free paths (MFP), denoted λ , and which arises from the interband part of the XAM. As well established in the Fuchs-Sondheimer theory [24, 25] of the resistivity of thin metal films, linear momentum non-conserving scattering processes at conductor boundaries, associated with atomic-scale surface roughness, leads to a transverse gradient in the longitudinal response to an electric field. This is confined in a narrow region at the conductor edges scaling with the MFP. Within this kinetic boundary layer, the longitudinal charge current density exhibits a quasi-exponential variation, reaching a value at the surface that is significantly reduced compared to the bulk, as shown in Fig.1(b). This is quantitatively captured by the Boltzmann equation controlling the longitudinal linear response in terms of f_n , the deviation of the electron distribution function in band n . It reads

$$\partial_{\mathbf{p}} \varepsilon_n \cdot \partial_{\mathbf{x}} f_n + (e\mathbf{E}) \cdot \partial_{\mathbf{p}} n_{FD}(\varepsilon_n) = C[\mathbf{f}], \quad (5)$$

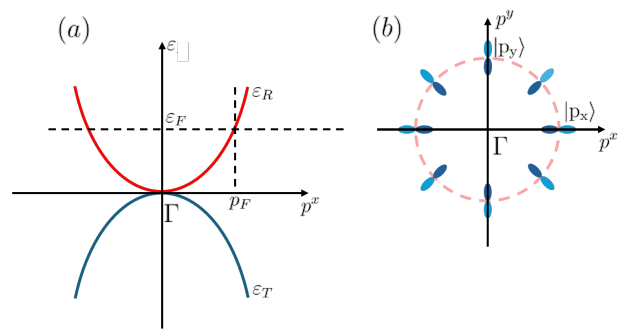


FIG. 2. (a) Schematic band structure of the R-T Hamiltonian model of two-dimensional (TR+I) symmetric metal considered in the text, for a concrete calculation of the interband XEA. A positive Fermi level intersects only the electron like band. (b) Radial p-orbital composition texture of the eigenstates on the Fermi line, for the electron like band.

with the RHS corresponding to the bulk disorder induced collision integral. Recently, Valet and Raimondi[23] have shown that such a spatial gradient in f_n can *locally* induce quantum coherences. In the present context, this gives rise to an additional contribution to the total XEA which, to the best of our knowledge, has not been previously considered. From Eq.(2) it is derived [33] as

$$X_{(ib)}^j = -\frac{\hbar}{2} \sum_{\substack{n \\ m \neq n}} \int_{BZ} \frac{d^d p}{(2\pi\hbar)^d} \partial_i f_n \text{Tr} \left[\hat{A}_{nm}^i \hat{X}_{mn}^j + \hat{X}_{nm}^j \hat{A}_{mn}^i \right], \quad (6)$$

in which $\hat{A}_{nm}^i = \mathbf{i} \partial_p^i \hat{P}_n \hat{P}_m$ is the non-Abelian interband Berry connection. In presence of SOI, this may lead to a new contribution to the SEA, as the spin operator may acquire interband components. More critically, Eq.(6) defines the sole OEA term which remains non-vanishing as the SOI approaches zero. Indeed, in this limit, the OAM operator becomes purely interband [33] and the possibility of intraband OAM transport disappears.

To gain further insights in this newly uncovered effect, which is likely to be the dominant contribution to the OEA in light transition metals with weak SOI, we perform a concrete calculation for a simple model of two-dimensional (2D) (TR+I) symmetric metal often introduced to illustrate orbital physics *i.e.*, the so-called radial-tangential (R-T) (p_x, p_y)-orbital model [14, 27, 28]. In the minimal version we choose to consider, the Hamiltonian matrix reads $\hat{h} = \varepsilon_R \hat{P}_R + \varepsilon_T \hat{P}_T$. As depicted in Fig.2(a), it comprises an electron like band $\varepsilon_R(\mathbf{p}) = p^2/(2m^*)$, and a hole like band $\varepsilon_T(\mathbf{p}) = -p^2/(2m^*)$, with m^* the electron effective mass, and with the pseudo-momentum \mathbf{p} confined in the (x, y) plane. We assume the Fermi level ε_F to be positive, so that it only intersects the electron like band. This band corresponds to eigenstates with a radial orbital composition *i.e.*, $\hat{P}_R = |R\rangle\langle R|$. With the momentum angle $\theta_{\mathbf{p}}$ implicitly defined by $\cos \theta_{\mathbf{p}} = p^x/p$ and $\sin \theta_{\mathbf{p}} = p^y/p$, we have $|R\rangle = \cos \theta_{\mathbf{p}} |p_x\rangle + \sin \theta_{\mathbf{p}} |p_y\rangle$, as illustrated in Fig.2(b) at the Fermi level. As for the

hole like band, it corresponds to eigenstates with a tangential orbital composition *i.e.*, $\hat{P}_T = |T\rangle\langle T|$ with $|T\rangle = -\sin\theta_{\mathbf{p}}|p_x\rangle + \cos\theta_{\mathbf{p}}|p_y\rangle$. Since we assume vanishing SOI, the twofold Kramers' degeneracy of the bands reduces to a pure spin degeneracy. One can then choose a global spin-quantization axis, allowing the spin degree of freedom to be entirely ignored. As for the OAM operator, adopting the atomic center approximation (ACA), we recognize that its only surviving component within the considered Hilbert space is the z component, *i.e.*, $\hat{L}^z = \hbar\hat{\tau}^y$, with $\hat{\tau}^y$ the y Pauli matrix acting over the $\{|p_x\rangle, |p_y\rangle\}$ orbital basis. This is to be expected for electrons whose orbital degrees of freedom are confined in the (x, y) plane. We assume zero temperature and a static disorder model consisting of an homogeneous dilute random distribution of point scalar potentials, treated at the level of the second Born approximation for the derivation of the collision integral on the RHS of Eq.(5). While we consider this system to be infinite in one direction in the plane, along which the electric field is applied, we assume a finite width W in the perpendicular direction. As a natural choice of boundary condition at the kinetic level, we consider the edges to perfectly randomize the linear momentum of the electrons upon backscattering. The sole dimensionless parameter determining the universal scaling behavior of the longitudinal response of this system, under the stated hypothesis, is then the Knudsen number defined as the ratio between the electron MFP at the Fermi level and the conductor width, *i.e.*, $\text{Kn} = \lambda/W$. In the experimentally relevant regime $\text{Kn} \ll 1$, and as further detailed in the Supplemental Material [33], one can derive an asymptotically accurate approximation for the electron longitudinal response, corresponding to a generalized electron hydrodynamic approximation [38] of the Fuchs-Sondheimer theory. Substituting this approximate solution of the Boltzmann equation (5) into Eq.(6), properly specialized for the considered system, we obtain

$$L^z = \frac{\hbar\Omega^z}{2\varepsilon_F}\hbar + O(\text{Kn}^3), \quad (7)$$

with $\Omega^z = (\partial_x\mathcal{J}_c^y - \partial_y\mathcal{J}_c^x)/e$ the *vorticity* associated with the electron particle current density \mathcal{J}_c/e . This equation deserves close consideration for its remarkable physical transparency. It makes manifest how the energy density associated with the vortical part of the *classical* electron flow, *i.e.*, $\hbar\Omega^z$, induces virtual quantum transitions across the interband energy gap $2\varepsilon_F$ at the Fermi surface, leading to a *local* quantum OAM density thanks to the interband character of \hat{L}^z . These virtual processes are made possible by the existence of a momentum dependence of the orbital composition of the eigenstates, as quantified by the interband Berry connection appearing in Eq.(6). At the considered level of asymptotic approximation of the longitudinal kinetics, the charge current density obeys the following generalized *electron hydrodynamic* equations

$$\partial_i\mathcal{J}_c^i = 0, \quad (8a)$$

$$\mathcal{J}_c^i = \sigma E^i + (\lambda/\sqrt{2})^2 \Delta\mathcal{J}_c^i, \quad (8b)$$

with σ is the conductivity, and in which $(\lambda/\sqrt{2})$ can be interpreted as the *vorticity* diffusion length [39], as induced here by disorder scattering. These equations need to be solved in accordance with boundary conditions (BCs) reflecting at the hydrodynamic level the assumed scattering properties of the edges [40]. In the present case, we obtain an impenetrability condition $\mathcal{J}_c^n|_{\Sigma} = 0$ and a slip boundary condition $\partial_n\mathcal{J}_c^t|_{\Sigma} = -\frac{2\pi}{3\lambda}\mathcal{J}_c^t|_{\Sigma}$, with \mathcal{J}_c^n and \mathcal{J}_c^t the normal and tangential components of the current, and ∂_n the normal derivative. After solving Eqs.(8) for the considered geometry, the current density profile reads

$$\mathcal{J}_c^x(y) = \left\{ 1 - \mathcal{B} \frac{\cosh\left[\frac{y}{(\lambda/\sqrt{2})}\right]}{\cosh\left[\frac{(W/2)}{(\lambda/\sqrt{2})}\right]} \right\} (\sigma E). \quad (9)$$

in which it is assumed that the infinite dimension and the applied electric field are along the x direction, while the origin is taken in the middle of the ribbon conductor of width W in the y direction. In Eq.(9), $\mathcal{B} = [1 + \frac{3}{2\pi\sqrt{2}} \tanh(\frac{1}{\sqrt{2}\text{Kn}})]^{(-1)}$ is a BCs dependent numerical factor, with $\lim_{\text{Kn}\rightarrow 0}\mathcal{B} \approx 0.26$ in the present case. Substituting this expression into Eq.(7), we finally obtain the OAM profile as

$$L^z(y) = \frac{\hbar}{2\varepsilon_F} \frac{\sqrt{2}\mathcal{B}E}{\rho\lambda} \frac{\sinh\left[\frac{y}{(\lambda/\sqrt{2})}\right]}{\cosh\left[\frac{(W/2)}{(\lambda/\sqrt{2})}\right]} \hbar, \quad (10)$$

with $\rho = 1/\sigma$ the resistivity and with the factor $\rho\lambda$ being recognized as independent of the disorder strength. Quite remarkably, the *functional form* of this profile is identical to the OEA profile derived from the assumption of a diffusive OAM transport driven by OHE [21, 22], and is in qualitative agreement with the experimental findings of a quasi-exponential localization of OEAs of opposite signs at the two opposite edges of ribbon conductors [22]. However, and this is the critical difference with previous analysis, we have demonstrated that this is *not* an evidence of an OHE-driven diffusive OAM transport. In light transition metals, the intraband OAM transport is likely to be largely suppressed, and the OAM to be instead *locally* and continuously generated by the electron current vorticity through interband quantum processes, while being continuously absorbed by the lattice, leading to a steady state OEA near the edges, as given by Eq.(10) in the case of our toy model. This purely interband OAM does *not* diffuse, in agreement with some earlier numerical findings from ab-initio calculations [41]. Its spatial extent is of the order of the MFP as depicted in Fig.1(b), hence *not* scaling with a purported OAM diffusion length. This prediction appears to be in reasonable agreement with the experimentally measured OEA layer thickness in Cr [21] and Ti [22] thin films, both of the order of 7 nm, which is close to what is expected for the MFP in these transition metals at room temperature. While we have confirmed a diffusion-like profile for the OEA, what is diffusing is *not* the OAM, but its *local* source, *i.e.*, the classical electron flow vorticity.

In conclusion, we have derived a new quantum kinetic theory of XHE and XEA in (TR+I) symmetric metals. We have demonstrated that physical spin and orbital currents shall be defined as intraband currents, leading to a unified formulation of the intrinsic XHE controlled by the non-Abelian Berry curvature. Except in the rare case of orbital degeneracy beyond Kramers' theorem, our findings demonstrate that, contrary to widespread assertions, the intrinsic OHE is not independent of SOI; rather, it is intrinsically a second-order effect in its strength. We have identified a new interband mechanism by which an XAM density can be locally generated by gradients in the longitudinal linear response to an electric field, which are ubiquitous near conductor boundaries and interfaces. This new effect is likely to dominate the field induced OEA in light (TR+I) metals, and we have shown that for a simple isotropic metal model it can be understood as the local generation of quantum OAM by virtual interband transitions induced by the electron classical flow vorticity. The explicit expressions derived from this model reproduce the qualitative features of recent OEA observations, while predicting a confinement within a few MFPs of the boundaries, which seems also compatible with experimental findings. We shall stress that while we have adopted an ACA definition of the OAM operator in the treatment of this simple model, none of our general results depends on this. Indeed, the alternate definition of the electron OAM [16, 17, 42], in the spirit of the modern theory of orbital magnetization [43–45], also results in an OAM operator becoming purely interband for (TR+I) symmetric metals with Kramers' twofold degenerate bands in the vanishing SOI limit [33], hence leading to all the same conclusions. We also outline that the newly identified XEA effect is entirely distinct from quantum interference effects previously considered by other authors [17, 27, 46], which may only affect the OEA within few atomic layers.

Beyond a major upheaval in the interpretation of OEA experimental observations, our framework opens a new chapter in the theoretical approach to orbitronics, in which for instance all previous computations of intrinsic XHE conductivities, their vertex corrections and other OAM transport coefficients (relaxation time, diffusion constant, boundary relaxation parameters) shall be computed anew from ab-initio derived band structure models of materials of interest, now with proper expressions. Looking past orbitronics *per se*, we want to stress that our work provides the theoretical foundation to open a new era of *electron flow gradient engineering*. Indeed, one can compute with our Eq.(6) the interband spin density locally induced in materials with SOI, by electron flow gradients controlled through modifications in adjacent layers or at interfaces. This provides for instance, and for the first time, an explicit first-principle formulation of the spin-vorticity coupling [47–50] for electrons in crystals. We believe that several recent experiments in metal-metal [51, 52], metal-semiconductor [53] and metal-oxide [54] hetero-structures shall be considered anew from this point-of-view, even so one shall not completely discount the possibility of (intraband) diffusion of OAM generated by orbital Edelstein effects at interfaces [55–57].

ACKNOWLEDGMENTS

We thank Albert Fert, Mairbek Chshiev, Mikhail Titov, Gerrit E.W. Bauer, Paul J. Kelly, Dimitrie Culcer, Armando Pezo and Xavier Waintal for fruitful discussions. This research has been supported by the EIC Pathfinder OPEN Grant No. 101129641 “OBELIX” and a France 2030 government grant managed by the French National Research Agency PEPR SPIN Grant No. ANR-22-EXSP0009 (SPINTHEORY).

-
- [1] J. Sinova, S. O. Valenzuela, J. Wunderlich, C. H. Back, and T. Jungwirth, Spin Hall effects, *Rev. Mod. Phys.* **87**, 1213 (2015).
 - [2] A. Soumyanarayanan, N. Reyren, A. Fert, and C. Panagopoulos, Emergent phenomena induced by spin-orbit coupling at surfaces and interfaces, *Nature* **539**, 509 (2016).
 - [3] B. A. Bernevig, T. L. Hughes, and S.-C. Zhang, Orbitronics: The intrinsic orbital current in *p*-doped silicon, *Phys. Rev. Lett.* **95**, 066601 (2005).
 - [4] D. Go, D. Jo, H.-W. Lee, M. Kläui, and Y. Mokrousov, Orbitronics: Orbital currents in solids, *Europhysics Letters* **135**, 37001 (2021).
 - [5] A. Manchon, J. Železný, I. M. Miron, T. Jungwirth, J. Sinova, A. Thiaville, K. Garello, and P. Gambardella, Current-induced spin-orbit torques in ferromagnetic and antiferromagnetic systems, *Rev. Mod. Phys.* **91**, 035004 (2019).
 - [6] T. G. Rappoport, First light on orbitronics as a viable alternative to electronics, *Nature* **619**, 38 (2023).
 - [7] K.-J. Lee, V. Cros, and H.-W. Lee, Electric-field-induced orbital angular momentum in metals, *Nature Materials* **23**, 1302 (2024).
 - [8] A. A. Rhonald Burgos Atencia and D. Culcer, Orbital angular momentum of bloch electrons: equilibrium formulation, magneto-electric phenomena, and the orbital hall effect, *Advances in Physics: X* **9**, 2371972 (2024).
 - [9] D. Jo, D. Go, G.-M. Choi, and H.-W. Lee, Spintronics meets orbitronics: Emergence of orbital angular momentum in solids, *npj Spintronics* **2**, 19 (2024).
 - [10] G. Y. Guo, S. Murakami, N. Nagaosa, and S.-C. Zhang, Intrinsic spin hall effect in platinum: First-principles calculation, *Physical Review Letters* **100**, 096401 (2008).
 - [11] J. Qiao, J. Zhou, Z. Yuan, and W. Zhao, Calculation of intrinsic spin hall conductivity by wannier interpolation, *Physical Review B* **98**, 214402 (2018).
 - [12] T. Tanaka, H. Kontani, M. Naito, T. Naito, D. S. Hirashima, K. Yamada, and J. Inoue, Intrinsic spin hall ef-

- fect and orbital hall effect in $4d$ and $5d$ transition metals, Phys. Rev. B **77**, 165117 (2008).
- [13] H. Kontani, T. Tanaka, D. S. Hirashima, K. Yamada, and J. Inoue, Giant orbital Hall effect in transition metals: Origin of large spin and anomalous Hall effects, Phys. Rev. Lett. **102**, 016601 (2009).
- [14] D. Go, D. Jo, C. Kim, and H.-W. Lee, Intrinsic spin and orbital hall effects from orbital texture, Phys. Rev. Lett. **121**, 086602 (2018).
- [15] D. Jo, D. Go, and H.-W. Lee, Gigantic intrinsic orbital hall effects in weakly spin-orbit coupled metals, Phys. Rev. B **98**, 214405 (2018).
- [16] A. Pezo, D. García Ovale, and A. Manchon, Orbital Hall effect in crystals: Interatomic versus intra-atomic contributions, Phys. Rev. B **106**, 104414 (2022).
- [17] O. Busch, I. Mertig, and B. Göbel, Orbital hall effect and orbital edge states caused by s electrons, Phys. Rev. Res. **5**, 043052 (2023).
- [18] C. Stamm, C. Murer, M. Berritta, J. Feng, M. Gabureac, P. M. Oppeneer, and P. Gambardella, Magneto-optical detection of the spin hall effect in pt and w thin films, Physical Review Letters **119**, 087203 (2017).
- [19] A. Pattabi, Z. Gu, J. Gorchon, Y. Yang, J. Finley, O. J. Lee, H. A. Raziq, S. Salahuddin, and J. Bokor, Direct optical detection of current induced spin accumulation in metals by magnetization-induced second harmonic generation, Applied Physics Letters **107**, 152404 (2015).
- [20] Y.-G. Choi, D. Jo, K.-H. Ko, D. Go, K.-H. Kim, H. G. Park, C. Kim, B.-C. Min, G.-M. Choi, and H.-W. Lee, Observation of the orbital hall effect in a light metal ti, Nature **619**, 52 (2023).
- [21] I. Lyalin, S. Alikhah, M. Berritta, P. M. Oppeneer, and R. K. Kawakami, Magneto-optical detection of the orbital Hall effect in chromium, Phys. Rev. Lett. **131**, 156702 (2023).
- [22] J. C. Idrobo, j. Rusz, G. Datt, D. Jo, S. Alikhah, D. Muradas, U. Noumbe, M. V. Kamalakar, and P. M. Oppeneer, Direct observation of nanometer-scale orbital angular momentum accumulation (2024), arXiv:2403.09269 [cond-mat].
- [23] T. Valet and R. Raimondi, Quantum kinetic theory of the linear response for weakly disordered multiband systems, Phys. Rev. B **111**, L041118 (2025).
- [24] K. Fuchs, Proc. Cambridge Philos. Soc. **34**, 100 (1938).
- [25] E. Sondheimer, Adv. Phys. **1**, 1 (1952).
- [26] R. E. Camley and J. Barnaś, Theory of giant magnetoresistance effects in magnetic layered structures with antiferromagnetic coupling, Phys. Rev. Lett. **63**, 664 (1989).
- [27] I. V. Tokatly, Orbital momentum hall effect in p -doped graphane, Phys. Rev. B **82**, 161404 (2010).
- [28] S. Han, H.-W. Lee, and K.-W. Kim, Orbital dynamics in centrosymmetric systems, Phys. Rev. Lett. **128**, 176601 (2022).
- [29] P. Tang and G. E. W. Bauer, Role of disorder in the intrinsic orbital hall effect (2024), arXiv:2401.17620 [cond-mat].
- [30] A. Graf and F. Piéchon, Berry curvature and quantum metric in n -band systems: An eigenprojector approach, Phys. Rev. B **104**, 085114 (2021).
- [31] J. Mitscherling, A. Avdoshkin, and J. E. Moore, Gauge-invariant projector calculus for quantum state geometry and applications to observables in crystals (2024), arXiv:2412.03637 [cond-mat.mes-hall].
- [32] T. Valet and R. Raimondi, Semiclassical kinetic theory for systems with non-trivial quantum geometry and the expectation value of physical quantities, EPL **143**, 26004 (2023).
- [33] See Supplemental Material at URL-will-be-inserted-by-publisher.
- [34] R. Shindou and K.-I. Imura, Noncommutative geometry and non-abelian berry phase in the wave-packet dynamics of Bloch electrons, Nuclear Physics B **720**, 399 (2005).
- [35] C. Xiao and Q. Niu, Conserved current of nonconserved quantities, Physical Review B **104**, L241411 (2021).
- [36] S. Murakami, N. Nagosa, and S.-C. Zhang, SU(2) non-abelian holonomy and dissipationless spin current in semiconductors, Phys. Rev. B **69**, 235206 (2004).
- [37] M. Gradhand, D. V. Fedorov, F. Pientka, P. Zahn, I. Mertig, and B. L. Györfy, First-principle calculations of the berry curvature of bloch states for charge and spin transport of electrons, Journal of Physics: Condensed Matter **24**, 213202 (2012).
- [38] I. V. Tokatly and O. Pankratov, Hydrodynamic theory of an electron gas, Physical Review B **60**, 15550 (1999).
- [39] J. Happel and H. Brenner, *Low Reynolds Number Hydrodynamics: With Special Applications to Particulate Media* (Martinus Nijhoff Publishers, The Hague, Netherlands, 1983).
- [40] J. C. Maxwell, On stresses in rarefied gases arising from inequalities of temperature and their diffusion by conduction, Philosophical Transactions of the Royal Society of London A **170**, 231 (1879).
- [41] M. Rang and P. J. Kelly, Orbital relaxation length from first-principles scattering calculations, Physical Review B **109**, 214427 (2024).
- [42] T. P. Cysne, S. Bhowal, G. Vignale, and T. G. Rapoport, Orbital hall effect in bilayer transition metal dichalcogenides: From the intra-atomic approximation to the bloch states orbital magnetic moment approach, Phys. Rev. B **105**, 195421 (2022).
- [43] T. Thonhauser, D. Ceresoli, D. Vanderbilt, and R. Resta, Orbital magnetization in periodic insulators, Phys. Rev. Lett. **95**, 137205 (2005).
- [44] D. Xiao, J. Shi, and Q. Niu, Berry phase correction to electron density of states in solids, Phys. Rev. Lett. **95**, 137204 (2005).
- [45] J. Shi, G. Vignale, D. Xiao, and Q. Niu, Quantum theory of orbital magnetization and its generalization to interacting systems, Phys. Rev. Lett. **99**, 197202 (2007).
- [46] J. Voss, I. A. Ado, and M. Titov, Orbital magnetization from interface reflections in a conductor with charge current, Phys. Rev. B **111**, L121402 (2025).
- [47] M. Matsuo, J. Ieda, K. Harii, E. Saitoh, and S. Maekawa, Mechanical generation of spin current by spin-rotation coupling, Physical Review B **87**, 180402(R) (2013).
- [48] M. Matsuo, Y. Ohnuma, and S. Maekawa, Theory of spin hydrodynamic generation, Physical Review B **96**, 020401(R) (2017).
- [49] R. Takahashi, M. Matsuo, M. Ono, K. Harii, H. Chudo, S. Okayasu, J. Ieda, S. Takahashi, S. Maekawa, and E. Saitoh, Spin hydrodynamic generation, Nature Physics **12**, 52 (2016).
- [50] D. Kobayashi, T. Yoshikawa, M. Matsuo, R. Iguchi, S. Maekawa, E. Saitoh, and Y. Nozaki, Spin current generation using a surface acoustic wave generated via spin-rotation coupling, Physical Review Letters **119**, 077202 (2017).
- [51] H. Nakayama, T. Horaguchi, C. He, H. Sukegawa,

- T. Ohkubo, S. Mitani, K. Yamanoi, and Y. Nozaki, Spin-torque generation using a compositional gradient at the interface between titanium and tungsten thin films, *Phys. Rev. B* **107**, 174416 (2023).
- [52] H. Nakayama, T. Horaguchi, J. Uzuhashi, C. He, H. Sukegawa, T. Ohkubo, S. Mitani, K. Yamanoi, and Y. Nozaki, Reversal of spin-torque polarity with inverting current vorticity in composition-graded layer at the ti/w interface, *Advanced Electronic Materials* **11**, 2400797 (2025).
- [53] T. Horaguchi, C. He, Z. Wen, H. Nakayama, T. Ohkubo, S. Mitani, H. Sukegawa, J. Fujimoto, K. Yamanoi, M. Matsuo, and Y. Nozaki, Nanometer-thick si/al gradient materials for spin torque generation, *Science Advances* **11**, eadr9481 (2025).
- [54] W. Gao, L. Liao, H. Isshiki, N. Budai, J. Kim, H.-W. Lee, K.-J. Lee, D. Go, Y. Mokrousov, S. Miwa, and Y. Otani, Nonlocal electrical detection of reciprocal orbital edelstein effect, arXiv preprint arXiv:2502.11040 [cond-mat.mes-hall] 10.48550/arXiv.2502.11040 (2025).
- [55] S. Krishnia, Y. Sassi, F. Ajejas, N. Reyren, S. Collin, A. Fert, J.-M. George, V. Cros, and H. Jaffrès, Large interfacial rashba interaction generating strong spin-orbit torques in atomically thin metallic heterostructures, *Nano Letters* **23**, 6785 (2023).
- [56] S. A. Nikolaev, M. Chshiev, F. Ibrahim, S. Krishnia, N. Sebe, J.-M. George, V. Cros, H. Jaffrès, and A. Fert, Large chiral orbital texture and orbital edelstein effect in Co/Al heterostructure, *Nano Letters* **24**, 13465 (2024).
- [57] S. Krishnia, B. Bony, E. Rongione, L. Moreno Vincente-Arche, S. Collin, A. Fert, J.-M. George, N. Reyren, V. Cros, and H. Jaffrès, Quantifying orbital rashba effect via harmonic hall torque measurements in transition-metal|cu|oxide structures, *APL Materials* **12**, 051105 (2024).